# Hypoxic tumor microenvironment activates GLI2 via HIF-1α and TGF-β2 to promote chemoresistance in colorectal cancer

Yen-An Tang[a,1], Yu-feng Chen[b,c,d,1], Yi Bao[a], Sylvia Mahara[a], Siti Maryam J. M. Yatim[a], Gokce Oguz[a], Puay Leng Lee[a], Min Feng[a], Yu Cai[e,f], Ern Yu Tan[g], Sau Shung Fong[g], Zi-huan Yang[c,d], Ping Lan[b,c,d], Xiao-jian Wu[b,c,d,2], and Qiang Yu[a,f,g,h,i,2]

[a]Cancer Therapeutics and Stratified Oncology, Genome Institute of Singapore, Agency for Science, Technology, and Research, Singapore 138672; [b]Department of Colorectal Surgery, The Sixth Affiliated Hospital, Sun Yat-sen University, Guangzhou 510655, China; [c]Guangdong Provincial Key Laboratory of Colorectal and Pelvic Floor Disease, The Sixth Affiliated Hospital, Sun Yat-sen University, Guangzhou 510655, China; [d]Guangdong Institute of Gastroenterology, The Sixth Affiliated Hospital, Sun Yat-sen University, Guangzhou 510655, China; [e]School of Pharmacy, Jinan University, Guangzhou 510632, China; [f]Cancer Research Institute, Jinan University, Guangzhou 510632, China; [g]Department of General Surgery, Tan Tock Seng Hospital, Singapore 308433; [h]Department of Physiology, Yong Loo Lin School of Medicine, National University of Singapore, Singapore 117597; and [i]Cancer and Stem Cell Biology, Duke-NUS Graduate Medical School, Singapore 169857

Edited by Gregg L. Semenza, Johns Hopkins University School of Medicine, Baltimore, MD, and approved May 21, 2018 (received for review January 24, 2018)

**Colorectal cancer patients often relapse after chemotherapy, owing to the survival of stem or progenitor cells referred to as cancer stem cells (CSCs). Although tumor stromal factors are known to contribute to chemoresistance, it remains not fully understood how CSCs in the hypoxic tumor microenvironment escape the chemotherapy. Here, we report that hypoxia-inducible factor (HIF-1α) and cancer-associated fibroblasts (CAFs)-secreted TGF-β2 converge to activate the expression of hedgehog transcription factor GLI2 in CSCs, resulting in increased stemness/dedifferentiation and intrinsic resistance to chemotherapy. Genetic or small-molecule inhibitor-based ablation of HIF-1α/TGF-β2–mediated GLI2 signaling effectively reversed the chemoresistance caused by the tumor microenvironment. Importantly, high expression levels of HIF-1α/TGF-β2/GLI2 correlated robustly with the patient relapse following chemotherapy, highlighting a potential biomarker and therapeutic target for chemoresistance in colorectal cancer. Our study thus uncovers a molecular mechanism by which hypoxic colorectal tumor microenvironment promotes cancer cell stemness and resistance to chemotherapy and suggests a potentially targeted treatment approach to mitigating chemoresistance.**

HIF | GLI2 | TGF-β | tumor microenvironment | chemoresistance

About 40 to 50% of stage II and stage III colorectal cancer (CRC) patients are resistant to therapy and have relapsed disease over the course of treatment (1). Cancer stem cells (CSCs) within the tumor mass have been proposed to mediate chemoresistance and metastatic progression (2–4). Recent attempts at molecular classifications of CRC have revealed that CRC subtypes enriched with stem-like/mesenchymal gene signatures represent highly aggressive CRCs (5–7). These findings have suggested therapeutically targeting CSCs as a potential strategy to block or attenuate the disease recurrence.

Although the investigation of resistance to therapy in CRC has been focused on genetic alterations or mechanisms intrinsic to cancer or CSCs, alternative views propose a role for paracrine signals received within the tumor microenvironment in promoting chemoresistance. In particular, recent studies have shown that stromal markers, rather than genes from epithelial tumors, associate robustly with disease relapse across the various classifications (8, 9). However, few studies exist to provide a clear mechanistic understanding of how tumor microenvironment induces chemoresistance.

Previous studies show that stromal factors secreted from cancer-associated fibroblasts (CAFs) such as Wnts, hepatocyte growth factor (HGF), or IL-17A contribute to the maintenance of colorectal CSCs and metastatic formation through activation of Wnt/β-catenin pathway (10–12). More recently, Guinney et al. (6) performed a comprehensive transcriptome analysis of publicly available gene expression data of CRC patients and identified four consensus molecular subtypes with distinguishing features. The most aggressive subtype is highly associated with both stromal infiltration and CSC gene signature, but not Wnt/β-catenin activation. The canonical subtype with Wnt activation, however, is not associated with CSC signature. This study highlights a possibility that colorectal CSCs are highly heterogeneous and may rely on alternative signaling(s) driven by stromal cells. Among the stromal factors, CRC-derived TGF-β has been shown to stimulate CAFs to secrete IL-11, which, in turn, confers metastatic capacity on CRCs by triggering GP130/STAT3 signaling (13). In line with these observations, TGF-β signaling was found to show enrichment in the poor-prognosis molecular CRC subtypes, and TGF-β–induced stromal gene expression programs are robust predictors of cancer recurrence and metastasis in CRC (5, 7, 8, 13). Although the above findings have identified a role for TGF-β stromal program in metastatic progression (14), it also remains unclear whether intrinsic resistance to

## Significance

**Colorectal cancer patients often relapse due to resistance to chemotherapy. The tumor microenvironment is known to contribute to tumor aggressiveness and chemoresistance, but the underlying mechanisms remain elusive. In the current study, we have shown that cancer-associated fibroblasts (CAFs) which are often present in the tumor can greatly promote resistance of colorectal cancer cells to chemotherapy. In the low-oxygen condition (hypoxia), CAFs-secreted growth factor TGF-β2 can induce strong expression of *GLI2*, a gene that can induce resistance to therapy. As such, therapeutic targeting of TGF-β and GLI2 can be developed into a useful adjuvant to enhance the effect of chemotherapies.**

Author contributions: Y.-A.T., X.-j.W., and Q.Y. designed research; Y.-A.T., Y.-f.C., Y.B., S.M., S.M.J.M.Y., P.L.L., and M.F. performed research; Y.-f.C., Y.C., E.Y.T., S.S.F., Z.-h.Y., P.L., and X.-j.W. contributed new reagents/analytic tools; Y.-A.T., Y.-f.C., Y.B., S.M., S.M.J.M.Y., G.O., and Q.Y. analyzed data; and Y.-A.T. and Q.Y. wrote the paper.

The authors declare no conflict of interest.

This article is a PNAS Direct Submission.



Data deposition: The data reported in this paper have been deposited in the Gene Expression Omnibus (GEO) database, https://www.ncbi.nlm.nih.gov/geo (accession nos. GSE93253 and GSE93254).

[1]Y.-A.T. and Y.-f.C. contributed equally to this work.

[2]To whom correspondence may be addressed. Email: wuxjian@mail.sysu.edu.cn or yuq@gis.a-star.edu.sg.

This article contains supporting information online at www.pnas.org/lookup/suppl/doi:10.1073/pnas.1801348115/-/DCSupplemental.

Published online June 11, 2018.

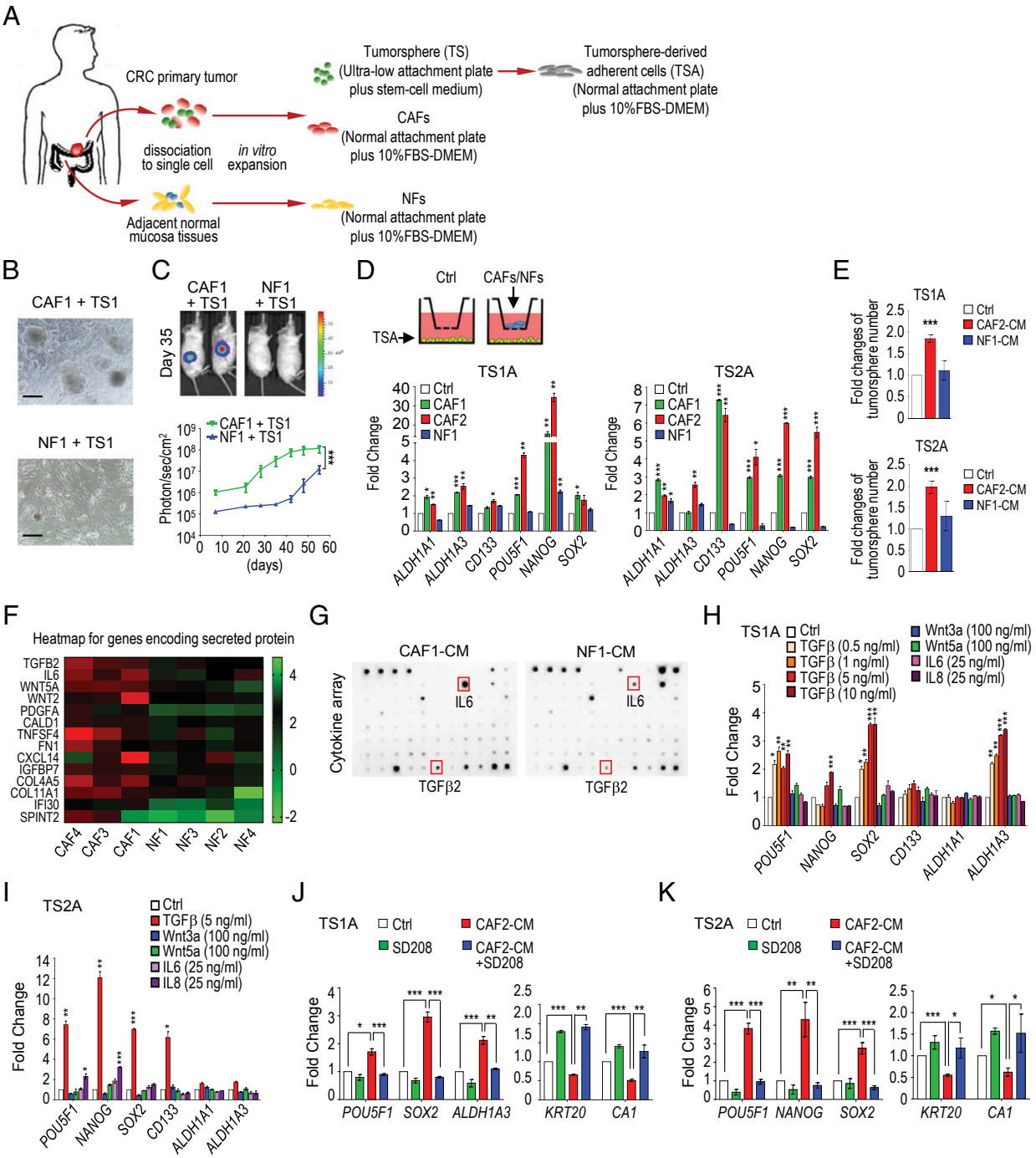


**Fig. 1.** Patient-derived CAFs-secreted TGF-β2 is essential for maintaining stemness of colorectal TSs. (*A*) Scheme depicting the establishment of TSs, CAFs, and NFs from disaggregated primary CRC samples. (*B*) Representative images of direct cell–cell contact coculture of TSs with CAFs or NFs. Phase-contrast microscopic images were photographed at day 37. (Scale bars, 100 μm.) (*C*) Representative bioluminescent imaging (BLI) showing the tumor growth of TS1-luc ($1 \times 10^3$ cells) coinjected with CAF1 or NF1 ($5 \times 10^4$ cells) into nonobese diabetic (NOD)/SCID mice at day 35 (*Top*). BLI curves are shown (*Bottom*; $n = 4$ for each group). (*D*) Quantitative PCR analysis is showing the relative gene expression in TSA cells separately cocultured with empty control (Ctrl) insert or CAFs/NFs. Scheme depicting the separate coculture setting (*Top*) and quantifications (*Bottom*). TS1A and TS2A refer to cancer cells derived from different patients. (*E*) In vitro TS formation assay of TSA cells with or without pretreatment of conditional medium (CM) from CAFs or NFs. (*F*) Heat map derived from expression microarray showing the 14 up-regulated genes encoding secreted proteins in CAFs compared with NFs. (*G*) Cytokine antibody array profiling of cytokine secretions in the CAF1 CM or NF1 CM. The framed dots indicate the location of TGF-β2 and IL-6. (*H* and *I*) Quantitative PCR analysis showing the relative gene expression in TSA cells treated with various recombinant cytokines for 48 h. (*J* and *K*) Quantitative PCR analysis of stemness genes (*Left*) and differentiation markers (*Right*) in (*J*) TS1A and (*K*) TS2A cells treated with CAF CM or together with 1 μM SD208 for 48 h. Quantifications are shown (*Right*; $n = 3$ for each group). Error bars represent SEM; $n = 3$. $^*P < 0.05$, $^{**}P < 0.01$, $^{***}P < 0.001$. *P* values were calculated with a two-tailed *t* test.

chemotherapy conferred by microenvironment utilizes shared or distinct molecular pathways. Intriguingly, exogenous treatment of TGF-β induces a cytostatic response rather than epithelial-to-mesenchymal transition phenotype in primary CRC tumors (8), leading to an unsolved question whether stromal TGF-β acts as promoting or suppressing factor toward colorectal CSCs.

Hypoxia, a critical feature in the tumor microenvironment, has been shown to promote cancer stemness through the hypoxia-inducible factors (HIFs) (15, 16). Previous studies demonstrated that the HIF-1α, but not HIF-2α, is elevated in CRC patients and is associated with poor prognosis (17, 18), suggesting a role of HIF-1α in CRC tumorigenesis, although how hypoxia along with CAFs preserves a CSC niche for maintenance of phenotype plasticity and chemoresistance is unclear. In this study, we addressed these questions by exploiting patient-derived in vitro and in vivo models and investigated the functional interplay between CAFs and CSCs. In particular, we asked whether and how a hypoxic environment assists CAFs/stromal TGF-β in promoting CSCs by switching the balance between stemness and differentiation state, which leads to cell survival and chemoresistance. Our study identifies a previously uncharacterized pathway that drives chemoresistance and reveals a treatment strategy to improve clinical outcomes of CRC.

## Results

**Investigation of Patient-Derived CAFs–CSC Interaction Identifies TGF-β2 as a Key Stromal Factor Promoting CRC Stemness.** To investigate the interplay between CAFs and colorectal CSCs, we isolated colorectal CSCs and CAFs from primary tumors of CRC patients and established several in vitro coculture model systems (Fig. 1*A*). As a control, we also isolated the normal fibroblasts (NFs) from the adjacent normal mucosa of CRC. Because of the heterogeneity of CSC markers in CRC (11, 19), we disassociated fresh surgical tumors into single-cell populations and cultured them as tumor spheroids in serum-free medium to model CSC as previously described (19) (named TS1, TS2, and TS3, isolated from different patients). Upon addition of FBS to the colorectal tumorsphere (TS) cultures, TS cells became adherent to the tissue culture plates, resulting in differentiation (named TS1A and TS2A). As expected, TS-derived adherent (TSA) cells showed reduced expression of known colorectal CSC markers (*CD133* and *ALDH1A1*) and CRC stemness genes (*POU5F1*, *NANOG*, and *SOX2*) (20, 21). In contrast, they showed increased expression of intestinal epithelial differentiation markers (*MUC2*, *KRT20*, *FABP2*, and *CEACAM7*) (*SI Appendix*, Fig. S1 *A* and *B*). Also, TSA cells showed much-reduced ALDH activity compared with TS cells (*SI Appendix*, Fig. S1 *C* and *D*). In vivo, serial dilutions experiment showed that the TS cells had a much more robust capacity to initiate tumor formation when engrafted into immunodeficient mice compared with TSA cells (*SI Appendix*, Fig. S1*E*). Thus, the TS cells derived from the CRC were confirmed to contain highly enriched CSC population and are highly tumorigenic. For CAFs, we verified that they expressed high levels of the CAF-specific maker, α-SMA, compared with NFs (*SI Appendix*, Fig. S1*F*). Moreover, immunocytochemistry staining verified the high expression of CAF-associated protein markers including α-SMA, vimentin, and fibronectin in CAFs compared with NFs (*SI Appendix*, Fig. S1*G*).

When CAFs and NFs derived from different patient tumors were cultured to contact with TS cells in a direct coculture system, we found that CAFs were able to support the spheroid growth of TS cells, but NFs did not seem to have this capacity (Fig. 1*B*). Importantly, engraftment of CAF–TS coculture into immunodeficient mice resulted in markedly more robust tumor initiation compared with NF–TS coculture (Fig. 1*C*). These findings from both in vitro and in vivo experiments demonstrated the ability of CAFs in supporting the tumorigenicity of colorectal cancer CSCs.

To investigate the ability of CAFs to modulate the equilibrium between stemness and differentiation of CRC cells, we further used an indirect coculture system in which TSA cells were cocultured with CAFs or NFs in a well insert to prevent the direct interaction of the two cell types (Fig. 1*D*). In this system, both CAF1 and CAF2 cells, but not NF cells, induced the expression of CSC markers and stemness genes in TS1A and TS2A cells (Fig. 1*D*) but reduced the expression of differentiation markers (*SI Appendix*, Fig. S2). Consistently, directly adding the conditioned medium (CM) of CAFs to the TSA cell culture led to the increased ability of TSA cells to form TSs, while CM of NFs failed to do this (Fig. 1*E*). These studies, through different approaches, demonstrate that the CAFs promote self-renewal and tumorigenicity of CSCs while inhibiting the differentiation capacity, and these effects are mediated through CAF-secreted protein(s)/factor(s).

To identify CAF-associated genes that encode secreted proteins to promote stemness, we performed a transcriptome analysis in CAFs and NFs and identified 269 genes up-regulated in CAFs compared with NFs. Among them, 14 genes are annotated to encode secreted proteins, including *TGF-B2*, *IL-6*, and *WNT5A* (Fig. 1*F*), and their differential expression between CAFs and NFs were further verified by qRT-PCR (*SI Appendix*, Fig. S3*A*). Further proteomic analysis of the conditional medium of CAFs and NFs using a cytokine antibody array identified TGF-β2 and IL-6 as top candidates that are secreted at a higher amount in CAF–CM compared with NF–CM (Fig. 1*G*). Moreover, among various recombinant cytokine proteins, TGF-β, given from 0.5 ng/mL to 10 ng/mL, was able to induce the expression of CSC markers and stemness genes (Fig. 1 *H* and *I*). However, the Wnt ligands (Wnt3a and Wnt5a) as well as interleukins (IL-6 and IL-8) failed to do so (Fig. 1 *H* and *I*). ELISA showed that the amount of secreted TGF-β2 protein from CAFs ranged from 1.0 ng/mL to 2.0 ng/mL (*SI Appendix*, Fig. S3*B*), indicating that the recombinant TGF-β we used to treat CSC was within the physiological range.

The role of TGF-β signaling in CAFs-induced stemness and dedifferentiation was further confirmed by using TGF-β receptor I inhibitor (TGFBRi; SD208) which effectively reversed CAF–CM-induced expression of stemness genes or reduced expression of differentiation genes (Fig. 1 *J* and *K*).

Previous studies have reported that growth factors such as HGF, OPN, or SDF-1 secreted from myofibroblasts in CRC can activate the Wnt/β-catenin signaling leading to CSC clonogenicity (10, 11). In our gene expression and cytokine antibody array analysis, these growth factors did not show differential expression between CAFs and NFs or CAF–CM and NF–CM. In contrast to Wnt3a, CAF–CM did not induce the β-catenin nuclear accumulation in TSA cells (*SI Appendix*, Fig. S3*C*) nor did it increase the β-catenin reporter activity (*SI Appendix*, Fig. S3*D*). The expression of Wnt/β-catenin target genes *LGR5* and *CD44v6* was also not affected by CAFs (*SI Appendix*, Fig. S3*E*). Therefore, we excluded the role of Wnt/β-catenin in our CAF–CSC model systems.

**CAFs-Secreted TGF-β2 Induces the *GLI2* Expression in CSCs, Independently of the Canonical Hedgehog Signaling.** To interrogate the downstream effectors of CAF-mediated TGF-β signaling in driving CSC, we transduced a retroviral vector expressing Red Fluorescent Protein (RFP) into TS cells and treated the TS or CAF–TS coculture with TGFBRi (SD208). The RFP-positive TS cells were then FACS-sorted and subjected to transcriptome analysis (Fig. 2*A*). We identified 610 genes up-regulated by CAFs but down-regulated by SD208, thus defined as "CAF–TGF-β activated gene set." Ingenuity Pathway Analysis (IPA) analysis of this gene set revealed numerous enriched gene networks, including a top-ranked embryonic development network which highlights the *GLI2*-associated Hedgehog pathway (Fig. 2 *B* and *C*). As an independent validation, we also used TGF-β to treat TS cells, and, again, the embryonic development network which contains the *GLI2*-associated Hedgehog pathway was found to be up-regulated by TGF-β (*SI Appendix*, Fig. S4*A*). Given the implications of Hedgehog signaling in multiple aspects of tumorigenesis, we chose to investigate a role of stromal TGF-β2 signaling in the regulation of *GLI* transcriptional factors, which are the key components of Hedgehog signaling. To first verify the effects of TGF-β on the Hedgehog pathway, recombinant TGF-β2 and other cytokines were used to treat TSA cells. The results showed that TGF-β treatment

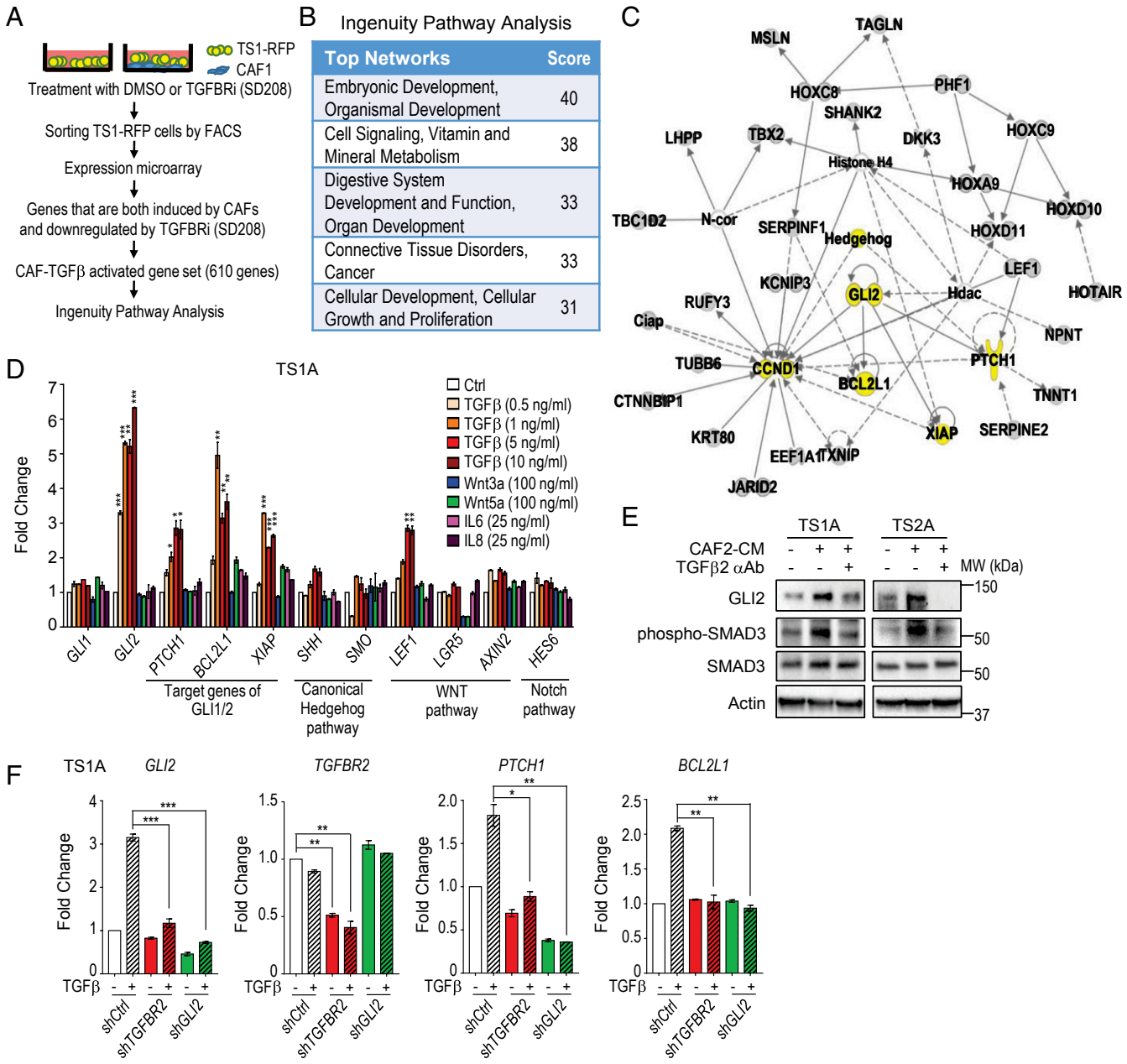


**Fig. 2.** CAF-secreted TGF-β2 induces GLI2 expression leading to activation of noncanonical Hedgehog pathway. (*A*) Scheme depicting the experimental design for the acquisition of CAF–TGF-β activated gene set using expression microarray. (*B*) IPA shows the five top-ranked networks enriched in the CAF–TGF-β activated gene set from *A*. (*C*) The network map of "Embryonic Development" from *B* involves GLI2-associated Hedgehog pathway (highlighted in yellow). (*D*) Quantitative PCR analysis showing the relative expression of indicated genes involving Hedgehog, Wnt, and Notch pathways in TS1A cells treated with various cytokines for 48 h. (*E*) Western blotting showing the indicated proteins in TS1A (*Left*) and TS2A (*Right*) cells treated with or without CAF CM or TGF-β2–neutralizing antibody for 48 h. (*F*) Quantitative PCR analysis showing the relative expression of indicated genes in TS1A–shCtrl, –shTGFBR2, or –shGLI2 cells treated with or without TGF-β for 48 h. Error bars represent SEM; $n = 3$. $^{*}P < 0.05$, $^{**}P < 0.01$, $^{***}P < 0.001$. *P* values were calculated with a two-tailed *t* test.

consistently induced the expression of *GLI2* as well as its downstream targets *PTCH1*, *BCL2L1*, and *XIAP*, but not the expression of *SMO* Hedgehog receptor and *SHH* Hedgehog ligand that activate the canonical Hedgehog pathway (Fig. 2*D* and *SI Appendix*, Fig. S4*B*). By contrast, Wnts or IL-6/IL-8 treatments did not induce the expression of *GLI2* and its downstream targets (Fig. 2*D*). Moreover, TGF-β treatment only induced modest or no effects on Wnt or Notch target genes (Fig. 2*D* and *SI Appendix*, Fig. S4*B*). These results indicate that TGF-β2 activates *GLI2* expression through a noncanonical activation of Hedgehog pathway without requiring the activation of Hedgehog ligand or receptor.

The role of TGF-β2 in activating the *GLI2* expression was further confirmed by using TGF-β2 neutralizing antibody which blocked the CAF–CM-induced GLI2 expression following the activation of TGF-β–Smad signaling (Fig. 2*E*). Similarly, knockdown of *TGFBR2* (encoding TGF-β receptor II) or *GLI2* decreased TGF-β2–induced *GLI2* expression and its downstream targets *PTCH1* and *BCL2L1* (Fig. 2*F*). We next performed immunohistochemistry (IHC) analysis and validated the positive correlation of α-SMA (a known CAF marker), TGF-β2, and GLI2 proteins in the tissue microarray (TMA) which consists of tumor specimen of 245 CRC patients (*SI Appendix*, Fig. S4 *C* and *D*). Together, these findings confirm that CAF-secreted

TGF-β2 plays a crucial role in up-regulating GLI2 expression in CRC in vitro and in vivo.

**Hypoxia Cooperates with CAF to Further Induce the *GLI2* Expression Through a Cooperative Effect of HIF-1α and TGF-β2.** To determine the clinical relevance of CAF–TGF-β activated gene set, we analyzed the public gene expression data of CRC tumors from patients with documented information on clinical recurrence (22). Gene set enrichment analysis (GSEA) analysis showed that the CAF–TGF-β activated gene set was highly enriched in genes positively associated with CRC recurrence ($P < 0.001$; FDR < 0.001, Fig. 3*A*). When using hallmark gene set analysis of GSEA, we found that "hypoxia signature," in addition to the "TGF-β signature," was top-ranked in association with the CRC recurrence (Fig. 3 *B* and *C*). Given that hypoxic microenvironment is known to correlate with chemoresistance (23), we reasoned a possible role for hypoxia in CAF-mediated TGF-β2–GLI2 activity in inducing chemoresistance and tumor recurrence.

Validating this hypothesis, we first found that hypoxia was able to induce the expression of the GLI2 protein in TS cells cocultured with CAFs, as assessed by immunostaining (Fig. 3*D*). Furthermore, TS cells exposed to hypoxia showed increased *GLI2* mRNA expression, which was further elevated upon the TGF-β treatment (Fig. 3*E*). Moreover, Western blot analysis confirmed that TGF-β treatment in hypoxia resulted in a further induction of GLI2 (Fig. 3*F*). These data indicated a coordinated action of TGF-β and hypoxia for *GLI2* induction.

To verify whether hypoxia and TGF-β signaling directly regulate *GLI2* transcription, we performed immunoprecipitation (ChIP)-PCR analysis to determine the recruitment abundance of HIF-1α and SMAD3 at the *GLI2* promoter. The data showed that HIF-1α protein was recruited to the *GLI2* promoter at −484 to ∼−374 [P2 region containing a consensus hypoxia response element (HRE) 5′-ACGTG-3′ or 5′-GCGTG-3′] upon hypoxia treatment, independently of TGF-β treatment (Fig. 3*G*, *Left*). SMAD3 protein, the downstream transcriptional effector of TGF-β signaling, was also recruited to the *GLI2* promoter at −484 to ∼−374 (P2) and −196 to ∼−82 (P3) in response to TGF-β treatment, regardless of hypoxia or normoxia (Fig. 3*G*, *Right*). Finally, *GLI2* gene reporter assay demonstrated that *GLI2* promoter region flanking the three putative HREs was responsive to a stabilized form of HIF-1α, while the region lacking the HRE did not show a response to HIF-1α (Fig. 3*H*). Moreover, when these HREs were mutated, they were no longer responsive to HIF-1α (Fig. 3*H*). Collectively, these findings suggest that HIF-1α regulates *GLI2* expression through direct binding to the HREs in the *GLI2* promoter. This effect synergizes with TGF-β (through Smad3) but does not seem to require physical interaction between the two proteins, as we failed to detect an interaction of HIF-1α with SMAD3 by coimmunoprecipitation assay.

Furthermore, consistent with the induction of GLI2 by hypoxia, we detected increased expression of GLI2 target genes such as *BCL2L1*, *PITCH1*, and *XIAP* (*SI Appendix*, Fig. S5*A*). Hypoxia also induced the expression of stemness genes as well as enhancing the TS-forming capacity in a GLI2-dependent manner (*SI Appendix*, Fig. S5 *B* and *C*), consolidating a functional role of hypoxia-induced GLI2 in inducing stemness.

**Hypoxia and CAFs Promote a Robust Resistance to Chemotherapy in a GLI2-Dependent Manner.** We next investigated whether CAF–TS interaction, particularly in hypoxic condition, promotes chemoresistance. To this end, we stably transfected the TS cells with luciferase reporter so their viability could be measured specifically toward TS cells in the coculture. First, we found, as expected, that TSA cells compared with TS cells were more sensitive to clinically used FOLFOX regimen (combination of 5-Fu and Oxaliplatin) (Fig. 4*A*). Upon coculture with CAF, both TS and TSA cells showed increased resistance to chemotherapy (Fig. 4*A*). Similarly, treatment of TS cells with CAF–CM or TGF-β2, but not IL-6, Wnt3a, and Wnt5a, led to chemoresistance (Fig. 4*B*). Moreover, hypoxia markedly boosted the resistance of TS cells to chemotherapy upon coculture with CAFs (Fig. 4*C* and *SI Appendix*, Fig. S6*A*). Nevertheless, compared with the normoxia condition, hypoxia only showed a modest effect on TS1 and TS2 cells without CAFs (Fig. 4*C* and *SI Appendix*, Fig. S6*A*). This observation suggests that hypoxia and CAFs coordinate to promote a greater level of resistance to chemotherapy. Importantly, three independent *GLI2* knockdowns ablated CAF-mediated chemoresistance in both normoxia and hypoxia in TS and TSA cells (Fig. 4*D* and *SI Appendix*, Fig. S6*B*), suggesting a crucial role for GLI2 in CAF-induced chemoresistance. Of note is that, although hypoxia also induced the expression of HIF-2α (*SI Appendix*, Fig. S6*C*), HIF-2α knockdown did not reduce CAF/hypoxia-mediated chemoresistance (*SI Appendix*, Fig. S6*D*). In contrast, HIF-1α knockdown largely diminished the chemoresistance (Fig. 4*E* and *SI Appendix*, Fig. S6*E*).

Conversely, ectopic overexpression of GLI2 in TS cells in normoxia to a level similar to that seen in hypoxia resulted in a comparable induction of its downstream antiapoptotic target BCL-$_{X}$L, resulting in chemoresistance in TS–CAF coculture, resembling the CAF–TS coculture in hypoxia (Fig. 4*F*). Furthermore, ectopic overexpression of GLI2 in *HIF-1A*–depleted cells was sufficient to rescue the BCL-$_{XL}$ level and restored the hypoxia-induced chemoresistance (Fig. 4*G*); it also restored the resistance of *TGFBR2*-depleted cells to chemotherapy in both normoxia and hypoxia (*SI Appendix*, Fig. S6 *F* and *G*). Of note is that, although *TGFBR2* depletion in TS cells was sufficient to reduce CAF-mediated chemoresistance in normoxia, this effect was much smaller in hypoxia (*SI Appendix*, Fig. S6*H*). Together, these experiments established a crucial and indispensable role for GLI2 in driving chemoresistance ascribed to two different tumor microenvironmental cues, CAFs, and hypoxia.

**Combination of TGF-β Inhibitor SD208 and GLI Inhibitor GANT61 Reverses Chemoresistance Effectively.** To explore small molecule inhibitors of TGF-β/GLI2 pathway to reverse chemoresistance, we used GANT61, an inhibitor in preclinical development that can block the DNA binding activity of GLI1/2 transcription factors, as well as the TGF-β inhibitor SD208. As expected, TS cells grown in the CAF–CM and treated with GANT61 or SD208 both showed reduced expression of CSC genes and stemness markers (Fig. 5*A* and *SI Appendix*, Fig. S7*A*). However, only SD208, not GANT61, was able to induce the differentiation markers (Fig. 5*B* and *SI Appendix*, Fig. S7*B*). This suggests that TGF-β signaling, in addition to routing through GLI2 to modulate a survival/apoptosis event, also affects the cell differentiation. Moreover, we found that, while TGF-β/hypoxia treatment antagonized chemo-induced poly(ADP-ribose) polymerase (PARP) cleavage and caspase 3 activation, GANT61 yielded the opposite effect (*SI Appendix*, Fig. S7*C*), supporting a role for TGF-β/GLI2 in modulating apoptosis. We thus reasoned that combination of GANT61 and SD208, which targets both GLI2-mediated prosurvival effect and TGF-β–mediated dedifferentiation effect, might yield a synergistic effect in combating microenvironment-induced chemoresistance. Indeed, the combination of the two small-molecule inhibitors markedly resensitized the TS1 and TS2 cells to chemotherapy in the presence of CAFs and hypoxia, which was very robust compared with SD208 or GANT61 alone (Fig. 5 *C* and *D*). For a comparison, SD208 combination with GDC0449, the canonical Hedgehog pathway inhibitor which targets SMO receptor, did not produce a synergistic effect (Fig. 5 *C* and *D*).

To validate the above findings in vivo, we made use of two patient-derived xenografts (PDX) mouse models that expressed different levels of TGF-β2/HIF-1α/GLI2. The CT34 PDX expressed much lower levels of HIF-1α, TGF-β2, and GLI2 proteins compared with the CT128 model, as assessed by both Western blot and ELISA (Fig. 5 *E* and *F*). Consistently, CT34 PDX was responsive to FLOFOX treatment in vivo (Fig. 5*G*), while CT128 PDX was more resistant to chemotherapy but responsive to the combined treatment of chemotherapy with SD208 and GANT61 (Fig. 5*H*). Moreover, CT34 PDX tumor which has acquired resistance to chemotherapy through three rounds of chemo treatment in vivo (*SI Appendix*, Fig. S7*D*) showed enhanced expression of TGF-β2/HIF-1α

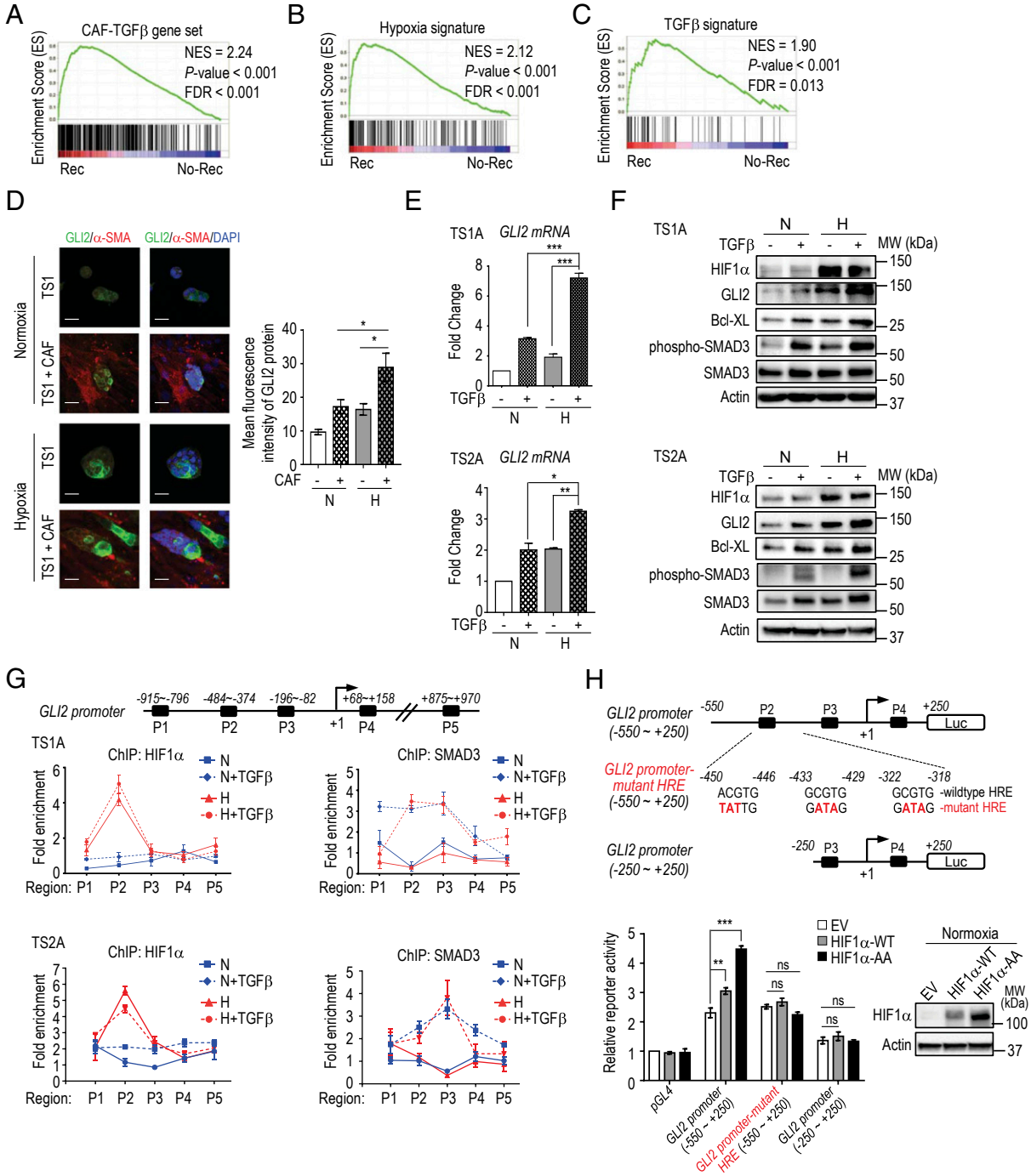


**Fig. 3.** HIF-1α and TGF-β2 cooperate to induce further GLI2 expression. (*A*) GSEA results showing the robust enrichment of CAF–TGF-β activated gene set obtained from Fig. 2*A* in recurrent (Rec) CRC patient samples compared with nonrecurrent (No-Rec) CRC samples. NES, normalized enrichment score. (*B* and *C*) GSEA results showing the strong enrichment of (*B*) hypoxia signature or (*C*) TGF-β signature in recurrent compared with nonrecurrent CRC patient samples. (*D*) Representative images of immunofluorescence assay showing the staining of indicated proteins or nucleus (DAPI) in TS1–CAFs coculture under normoxia or hypoxia (4% $O_2$) for 24 h (*Left*). Quantification of fluorescence intensity of GLI2 protein (*Right*). (Scale bars, 50 μm.) (*E*) Quantitative PCR showing the relative expression of *GLI2* in TS1A (*Top*) and TS2A (*Bottom*) cells treated with or without TGF-β2 in normoxia (N) or hypoxia (H; 4% $O_2$) for 48 h. (*F*) Western blotting showing the indicated proteins in TS1A (*Top*) and TS2A (*Bottom*) cells treated with or without TGF-β (10 ng·mL$^{-1}$) in normoxia or hypoxia (4% $O_2$) for 48 h. (*G*) Quantitative ChIP-PCR assay showing the occupancy of HIF-1α (*Left*) or SMAD3 (*Right*) protein at the different regions of the *GLI2* promoter in TS1A and TS2A cells treated with or without TGF-β2 (10 ng·mL$^{-1}$) under normoxia or hypoxia (4% $O_2$) for 24 h (*Bottom*). Scheme depicting the regions where primers were designed for amplifying across *GLI2* promoter (*Top*). (*H*) Dual-luciferase reporter assay showing the *GLI2* promoter activity in response to overexpression of HIF-1α using 293T cells under normoxia condition (*Bottom Left*). Scheme depicting the designs of *GLI2* promoter regions, which contain three wild-type or mutant HREs (*Top*). Western blot showing the expression levels of wild-type (WT) or stabilized P402A/P564A double-mutant (AA) of HIF-1α proteins (*Bottom Right*). Error bars represent SEM; $n = 3$. $^*P < 0.05$, $^{**}P < 0.01$, $^{***}P < 0.001$; n.s., not significant. *P* values were calculated with a two-tailed *t* test.

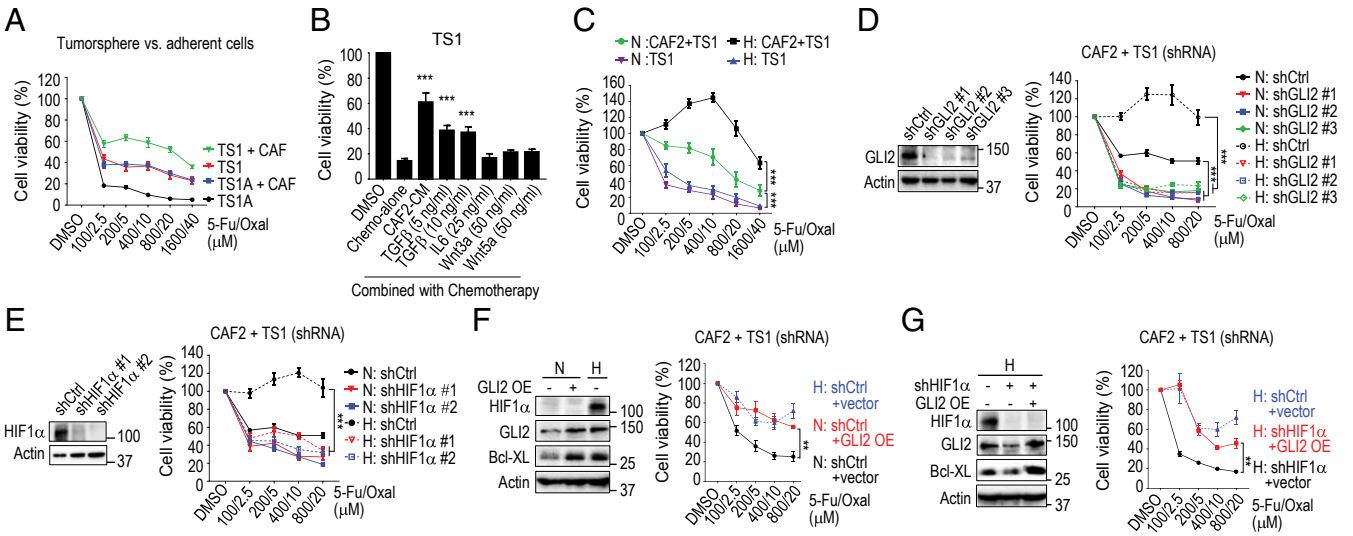


**Fig. 4.** Hypoxic and CAFs cooperate to induce robust chemoresistance in GLI2-dependent manner. (*A*) Cell viability of TS1-luc or TS1A-luc cells, which were cocultured with or without CAFs for 72 h, followed by treatment with indicated doses of combined chemotherapy reagents (5-Fu, 5-fluorouracil; Oxal, Oxaliplatin) for an additional 72 h. (*B*) Cell viability of TS1-luc cells, which were left untreated or treated with CAF CM or indicated cytokines for 7 d, followed by treatment with chemotherapy reagents (200 μM 5-Fu and 5 μM Oxal) for an additional 5 d. (*C*) Cell viability of TS1-luc cells, which were cocultured with or without CAFs in normoxia or hypoxia for 7 d, followed by treatment with combined chemotherapy reagents for an additional 5 d. (*D* and *E*) Western blot and cell viability of TS1-luc–shCtrl, three independent shGLI2 (*D*), or two independent shHIF-1A (*E*). (*F*) TS cells with or without GLI2 ectopic overexpression (OE) cocultured with CAFs in normoxia or hypoxia for 3 d, followed by treatment with chemotherapy for an additional 3 d: Western blot (*Left*) and viability (*Right*). (*G*) Western blot and cell viability of TS1-luc–shCtrl or TS1-luc–shHIF1A cells, with or without GLI2 ectopic overexpression cocultured with CAFs in hypoxia for 3 d, followed by treatment with chemotherapy for an additional 3 d (*Right*). Error bars represent SEM; $n = 3$. $^{**}P < 0.01$, $^{***}P < 0.001$. *P* values were calculated with a two-tailed *t* test.

and GLI2 (*SI Appendix*, Fig. S7 *E* and *F*). Collectively, our findings gathered from both in vitro and in vivo studies indicate that the level of TGF-β2/HIF-1α/GLI2 signaling is strongly associated with chemoresistance and that dual inhibition of TGF-β and GLI2 might be a useful approach to antagonizing chemoresistance in CRC.

**HIF-1α/TGF-β2/GLI2 Expression Is Associated with Relapse and Defines CRC Outcomes.** We next sought to determine whether the newly identified resistance pathway is of relevance to patient outcome. To this end, we made the use of a TMA which consists of tumor specimens of 245 stage II and stage III Chinese CRC patients with up to 7 y of follow-up information (24). We performed immunohistochemistry (IHC) analysis of GLI2, HIF-1α, and TGF-β2 proteins (Fig. 6*A*). As expected, GLI2 expression level showed significant correlation with HIF-1α (Pearson's $r = 0.706$; $P < 1.0 \times 10^{-6}$) or TGF-β2 (Pearson's $r = 0.684$; $P < 1.0 \times 10^{-6}$) (Fig. 6*B*), validating the association of GLI2 with HIF-1α/TGF-β2 in clinical CRC samples. Moreover, tumors from patients who later recurred after chemotherapy showed significantly higher expression of GLI2, HIF-1α, and TGF-β2 compared with tumors from patients who did not have a recurrence (Fig. 6*C*), indicating a correlation of GLI2 with relapse. Finally, Kaplan–Meier analysis of patient survival indicated that a higher level of GLI2 ($P = 4.0 \times 10^{-5}$), HIF-1α ($P = 0.0018$), or TGF-β2 ($P = 0.0023$) was strongly associated with poor disease-free survival (Fig. 6*D*). Remarkably, the combined expression of GLI2, HIF-1α, and TGF-β2 as a functional readout of this resistant pathway further enhanced the prognostic power in defining patients' disease-free survival outcome ($P = 9.0 \times 10^{-6}$) (Fig. 6*D*). Multivariate Cox regression analysis further demonstrated that the three-gene signature was an independent predictor of high-risk cancer relapse after adjusting for all of the clinicopathological characteristics (Fig. 6*E*).

To validate the above finding in different patients' cohorts, we further performed a metaanalysis consisting of four publicly available CRC gene expression databases (GSEGSE12945, GSE17538, GSE14333, and GSE31595) which covered a total of 621 CRC tumor samples. In this dataset, the expression of *GLI2* mRNA is also positively correlated with the expression of *TGFB2* (Pearson's $r = 0.2492$; $P = 3.40 \times 10^{-10}$), *HIF-1A* (Pearson's $r = 0.3846$; $P < 2.20 \times 10^{-16}$), or combined *TGFB2*/*HIF-1A* (Pearson's $r = 0.4274$; $P < 2.20 \times 10^{-16}$) (*SI Appendix*, Fig. S8*A*). Kaplan–Meier analysis of patient survival showed a strong prognostic power of *GLI2* ($P = 0.002$) or *TGFB2* ($P = 0.025$), although not *HIF-1A*, in disease-free survival (*SI Appendix*, Fig. S8*B*). Again, the combined expression of *GLI2*, *TGFB2*, and *HIF-1A* was much more robust in defining patients' disease-free survival outcome ($P = 1.9 \times 10^{-8}$) compared with a single gene or two-gene combination (*GLI2*/*TGFB2*) (*SI Appendix*, Fig. S8*B*). Moreover, further stratifying patients by different stages, the three-gene signature (*GLI2*/*TGFB2*/*HIF-1A*) consistently showed strong predictive power in both stage II ($P = 4.9 \times 10^{-6}$) and stage III ($P = 2.6 \times 10^{-4}$) patients (*SI Appendix*, Fig. S8*C*). Multivariate Cox regression analysis also showed that the three-gene signature was an independent predictor of high-risk cancer relapse (*SI Appendix*, Fig. S8*D*). In contrast, *GLI1* and *EPAS1* (encoding the HIF-2α protein) genes, either alone or in combination with *TGFB2*, failed to show a prognostic value (*SI Appendix*, Fig. S8 *E*–*H*). This analysis demonstrated the potential of our three-gene signature in prognostics of CRC.

## Discussion

We have described a mechanism of resistance in which the hypoxic tumor microenvironment regulates the plasticity of colorectal CSCs to escape the killing effect of chemotherapy (Fig. 6*F*). Our study is devoted to developing patient-derived models to dissect the microenvironmental interaction between hypoxia/CAFs and CSCs in a more clinically relevant system. It is different from many other studies that explore this topic by using immortalized NF or transformed cancer cell lines with limited clinical relevance.

CAFs are key players in the tumor microenvironment known to secrete compounds that potentiate tumor malignancy (25, 26). Although several recent studies have described stromal mechanisms promoting CRC metastasis, little is known about the signaling mechanisms of how CAFs are involved in empowering chemoresistance. It has been shown that stromal TGF-β promotes

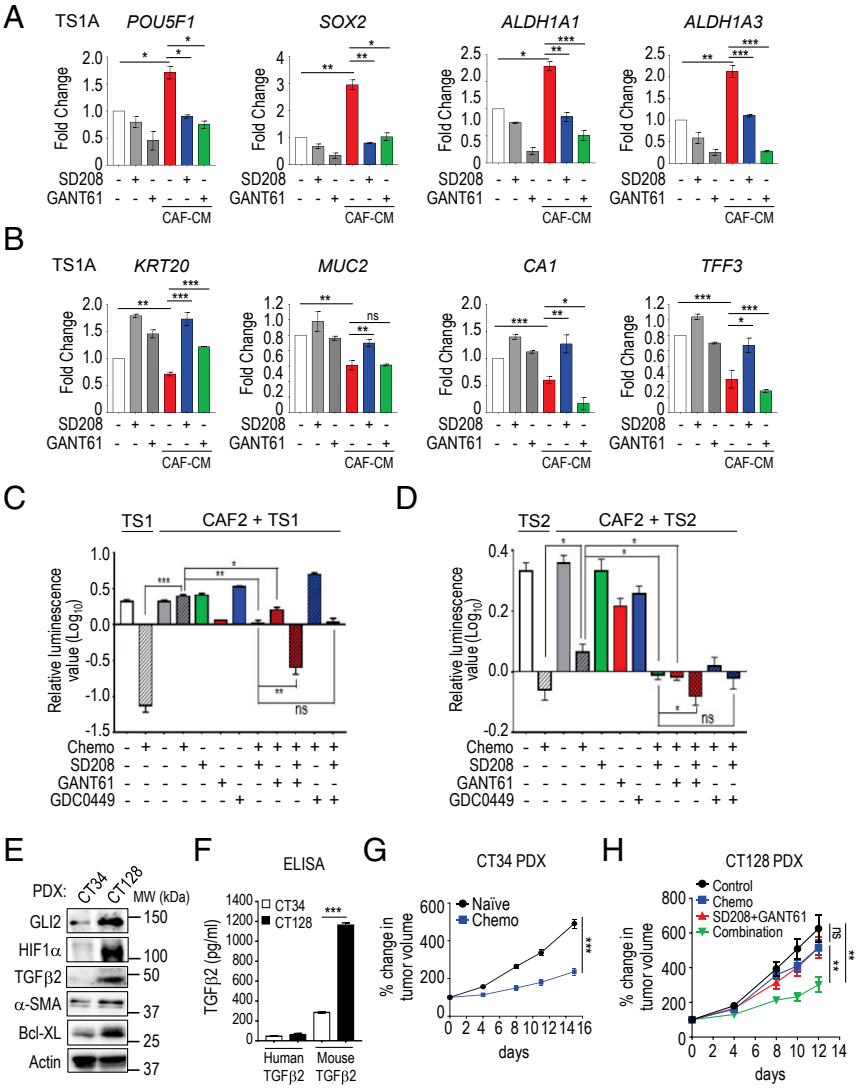


**Fig. 5.** Combination of SD208 and GNT61 effectively reverses tumor microenvironment-induced chemoresistance. (*A* and *B*) Quantitative PCR analysis showing the relative expression of indicated CSC and stemness genes (*A*) and differentiation markers (*B*) in TS cells treated with CAF CM together with or without 1 μM SD208 or 10 μM GANT61 for 48 h. (*C* and *D*) Relative cell viability of TS1-luc (*C*) or TS2-luc (*D*) cells, cocultured with or without CAFs and treated with single or combined inhibitor(s) (SD208, 1 μM; GANT61, 5 μM; GDC0449, 5 μM) in hypoxia for 7 d, followed by treatment with chemotherapy (Chemo: 200 μM 5-Fu; 5 μM Oxal) for 5 d. (*E*) Western blotting showing the indicated proteins in the CT34 or CT128 PDX tumors. (*F*) ELISA analysis showing the levels of human or mouse TGF-β2 proteins in the CT34 or CT128 PDX tumors. (*G* and *H*) The CT34 or CT128 PDX tumors were engrafted into nonobese diabetic (NOD)/SCID mice and left untreated or treated with two cycles of chemotherapy (5-Fu, 15 mg/kg; Oxal, 0.25 mg/kg) ($n$ = 9 for each group) or cotreated with SD208 (20 mg/kg) and GANT61 (50 mg/kg), or a combination (chemotherapy+SD208+GANT61) treatment ($n$ = 6 for each group). Error bars represent SEM; $n$ = 3. $^{*}P < 0.05$, $^{**}P < 0.01$, $^{***}P < 0.001$. $P$ values were calculated with a two-tailed $t$ test.

CRC metastasis through the activation of CAFs to stimulate the secretion of IL-11, resulting in activation of Stat3 in CRC (8, 13, 14). In this scenario, it has not yet been determined whether the mechanism associated with the metastatic trait is also relevant to chemoresistance. We demonstrated that CAFs-secreted TGF-β induced the expression of GLI2, an important effector of Hedgehog signaling, as a predominant pathway to promote CRC stemness and chemoresistance. On the other hand, we did not find that Wnt signaling was crucial in mediating the CAF-enhanced CSC activity in our models, although CAFs have been previously reported to promote the self-renewal activity of CSCs via Wnt pathway (10, 11). Unlike TGF-β, the addition of Wnt3a or Wnt5a failed to induce CSC genes or the expression of GLI2. We speculate that colorectal CSCs require the intrinsic activity of Wnt signaling for self-renewal which is only modestly regulated by the microenvironment.

Our results from the hypoxic coculture system yielded surprisingly robust results which indicate that tumor microenvironment contributes significantly to chemoresistance. Distinct from previous proposed drug-resistant mechanisms by hypoxia (23, 27), we show that this effect is through synergistic induction of *GLI2* expression by HIF-1α and CAFs-secreted TGF-β signaling, which is both required and sufficient to promote chemoresistance. Of note is that microenvironment-induced *GLI2* does not seem to be involved in the canonical Hedgehog pathway, which is different from *GLI1*, whose induction through canonical Hedgehog pathway has been recently associated with CRC spontaneous metastasis (28–30). Moreover, CAFs have been recently reported to secrete increased levels of cytokines, including TGF-β, to promote CSCs in the presence of chemotherapy (12), further highlighting the importance of TGF-β signaling in a hypoxic tumor environment to promote GLI2 expression and chemoresistance. In addition to a TGF-β2–induced GLI2 axis which might induce the escape of chemotherapy-induced apoptosis through induction of antiapoptotic targets such as BCL-$_{XL}$ and XIAP, TGF-β signaling also engages a distinct effector pathway to inhibit the differentiation of CSCs. The notion is further evidenced by the selective induction of differentiation marker following the TGF-β inhibition but not GLI2 inhibition. These data support the hypothesis that the two molecules converge and also coordinate to maintain both the self-renewal and survival of CSCs. That explains why a combined inhibition of both TGF-β and GLI2 is robust in inducing chemosensitization.

Given that hypoxia plays a major role in tumor progression and resistance to therapy, it represents a compelling therapeutic target for cancer treatment. Our GSEA analysis shows that hypoxia signature is the top-ranked hallmark gene set enriched in relapse CRC patients, which is also verified by in-house IHC analysis of HIF-1α protein which showed significant correlation with CRC recurrence. Although pharmaceutical targeting of HIF-1α or downstream of HIF-1α signalings, such as GLUT1, MCT1, and CA9, has been proposed to kill hypoxic tumor cells (23), it is still imperative to identify the most useful molecular targets in hypoxic

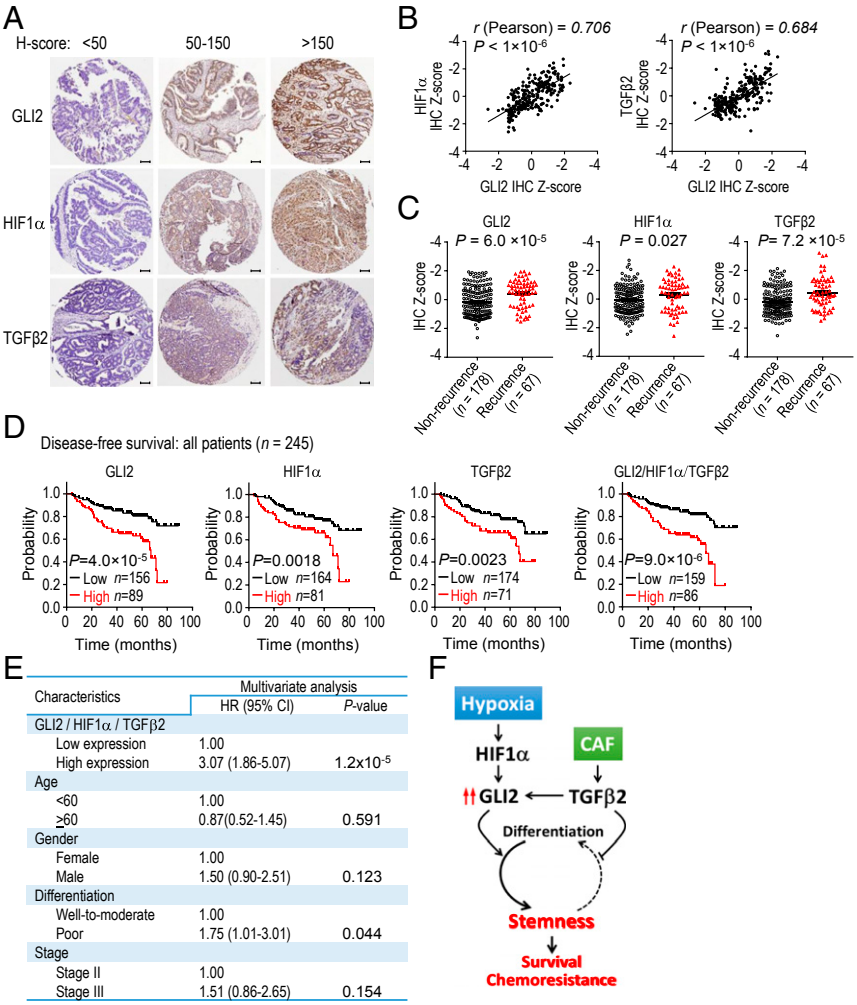


| Characteristics | Multivariate analysis | |
|---|---|---|
| | HR (95% CI) | *P*-value |
| GLI2 / HIF1α / TGFβ2 | | |
| Low expression | 1.00 | |
| High expression | 3.07 (1.86-5.07) | $1.2 \times 10^{-5}$ |
| Age | | |
| <60 | 1.00 | |
| ≥60 | 0.87(0.52-1.45) | 0.591 |
| Gender | | |
| Female | 1.00 | |
| Male | 1.50 (0.90-2.51) | 0.123 |
| Differentiation | | |
| Well-to-moderate | 1.00 | |
| Poor | 1.75 (1.01-3.01) | 0.044 |
| Stage | | |
| Stage II | 1.00 | |
| Stage III | 1.51 (0.86-2.65) | 0.154 |

**Fig. 6.** HIF-1α/TGF-β2/GLI2 expression signature defines CRC outcomes. (*A*) Representative IHC staining for GLI2, HIF-1α, and TGFB2 in TMAs. H scores for each TMA core were determined by the Slidepath Tissue IA software (Leica Microsystems). (Scale bars, 100 μm.) (*B*) The correlation of GLI2 protein level with HIF-1α or TGF-β2 protein levels from TMAs. The z score of GLI2 IHC intensity was plotted against that of HIF-1α or TGF-β2 IHC intensity ($n = 245$). (*C*) The z score of GLI2, HIF-1α, or TGF-β2 IHC intensity in tumor specimens from patients with or without recurrence. (*D*) Kaplan–Meier analyses of the association of disease-free survival with individual proteins or combined three-protein signature in 245 CRC patients from TMAs. (*E*) Multivariate Cox regression analysis of risk factors for cancer recurrence in CRC patients using IHC data of TMA. (*F*) The proposed model for the hypoxia/CAF–GLI2 axis in promoting colorectal CSC maintenance and chemoresistance. *P* values for correlation analyses (in *B*) were determined using Pearson's $\chi^2$ test; *P* values for survival analyses (in *D*) were determined using log-rank test; and P values in *C* were determined using two-tailed *t* test.

tumors. Thus, the combination with current standard of care cytotoxic therapy would have greater opportunity for cancer eradication. While the hypoxic tumors and microenvironment may represent a subpopulation in bulk tumors, the biggest challenge is to develop and improve the predictive tools of patient stratification for targeting hypoxic-related signaling pathways (23). Stratifying patients with CRC according to the gene expression profile of their tumor tissues has led to the development of multigene expression signatures, including gene expression signatures derived from stem cells and progenitor cells, for identifying high-risk colon cancer patients (6, 8, 22, 31–33). Although holding promise, these genomic assays may be difficult to implement and may not be sufficient to satisfy clinical need, due to the lack of a clear methodological "gold standard" to perform such analyses. We show that our three-gene signature, which is indicative of the activity of HIF-1α/TGF-β-GLI2 pathway, is robust in predicting a patient's outcome, which may provide an alternative approach for prognosis. We propose that these findings might be helpful in identifying patients who might be resistant to chemotherapy, although further validation in the framework of randomized clinical trials is required.

Therapeutically, some small-molecule inhibitors of TGF-β signaling are currently under clinical development for the treatment of different cancer types (34–36). In particular, the TGFBR inhibitor Galunisertib (LY2157299) has entered phase II/III clinical trial, and GLI1/2 inhibitor GANT61 has shown promising efficacy in numerous preclinical cancer models (37). Although their efficacy in humans is not yet known, our observations predict that pharmacological inhibition of both TGF-β signaling and GLI2 activity may yield activity to tackle chemoresistance and prevent CRC relapse in patients with enhanced expression of HIF-1α/TGF-β2/GLI2. Also, the proposed gene signature will help identify those patients more likely to benefit from the use of TGF-β inhibitors in future clinical trials. Future studies expanding the therapeutic potential of this newly identified pathway will have important clinical implications.

## Methods

**The Culture of Patient-Derived TSs and Fibroblasts.** Human biological samples used to expand TSs were obtained from individuals treated at the Sixth Affiliated Hospital of Sun Yat-sen University (Guangzhou, Guangdong, China), under informed consent and approval by the Ethics Committee of the

Sixth Affiliated Hospital, Sun Yat-sen University. All of the studies with these samples were approved by IRB for research purposes. The resected human colon tumors were minced and digested in 1 mg·mL$^{-1}$ of collagenase/dispase (Roche) in DMEM/F12 medium at 37 °C for 1 h, followed by erythrocytes depletion. Cells were then cultured in ultra-low attachment plate in CSC medium [serum-free DMEM/Ham's F-12, supplemented with B27, N2 (Invitrogen), 20 ng·mL$^{-1}$ of epidermal growth factor and 20 ng·mL$^{-1}$ of basic fibroblast growth factor, 0.5 μg·mL$^{-1}$ of hydrocortisone, and 4 μg·mL$^{-1}$ of heparin]. For the generation of TSA cells, the TS cells were dissociated to single cells, resuspended with DMEM (GIBCO) supplemented with 10% FBS, and plated in a normal six-well, flat-bottom plate. For isolation of primary fibroblasts, colorectal specimens and adjacent normal mucosa were minced and incubated with 1 mM EDTA at 37 °C for 30 min with repetitive shaking to remove epithelial cells. Samples were then digested enzymatically in 1 mg·mL$^{-1}$ collagenase/dispase at 37 °C for 1 h. Cells were then plated at high density with 10% FBS–DMEM. After six passages, the fibroblasts were harvested, and the total RNA was extracted for qRT-PCR analysis of universal fibroblasts markers. Details of reagents and methods used in this study can be found in *SI Appendix, Supplementary Materials and Methods*.

**Tissue Specimens.** Human CRC TMAs and resected CRC tissue samples for in vitro and in vivo PDX models were provided from the Sixth Affiliated Hospital, Sun Yat-sen University (24) and Tan Tock Seng Hospital. Studies with these samples were approved by institutional review boards: the Ethics Committee of the Sixth Affiliated Hospital, Sun Yat-sen University and National Healthcare Group Domain Specific Review Board (Singapore). Informed written consent had been previously obtained from each patient who agreed to provide tissue for research purposes.

**Assembly and Normalization of Gene Expression Array Databases Used for the Disease-Free Survival Analysis of Colorectal Cancer Patients.** The bioinformatics analysis of survival status with gene expression profile of four publicly available human gene expression array experiments downloaded from the National Center for Biotechnology Information (NCBI) Gene Expression Omnibus (GEO) database (GSE12945, GSE17538, GSE14333, and GSE31595). After downloading and cross-checking for duplications, all gene expression arrays were pooled, the batch effects were removed using ComBAT in R programming (38), and the arrays were transformed to z-score value by the formula: $Z = X - \mu/\sigma$ (where $X$ stands for gene expression value, $\mu$ stands for mean, and $\sigma$ stands for SD). For disease-free survival analysis, across four GEO datasets, there were 514 patients annotated with clinical information (GSE12945, $n = 51$; GSE17538, $n = 200$; GSE14333, $n = 226$; and GSE31595, $n = 37$). To stratified patients with high expression or low expression of an individual gene, the cutoff of z-score value was set as "mean + 1 standard deviation." For three-gene signature (*GLI2/TGFB2/HIF-1A*), the average of expression values from individual genes was used for z-score transformation as described above.

**Statistical Analysis.** All in vitro experiments were repeated at least three times unless stated otherwise, and the data are shown as mean ± SEM. For all in vitro experiments, $P$ values were calculated by either two-tailed Student's $t$ test or one-way ANOVA. For normalization of the expression of each patient cohort, expression values were normalized by calculating the z score across four GEO datasets. The disease-free survival curve of clinical patients was plotted using Kaplan–Meier analysis, and the statistical parameters were calculated by log-rank (Mantel–Cox) test using SPSS software. In all statistical tests, the resulting $P < 0.05$ was considered to be statistically significant.

**ACKNOWLEDGMENTS.** This work was supported by the core budget of the Agency for Science, Technology, and Research of Singapore, Singapore-China Collaborative Research Grant 13-711102 (to Q.Y. and X.-j.W.), International S&T Cooperation Program of China Grant 2013DFG32990 (to X.-j.W. and Q.Y.), and National High Technology Research and Development Program (863) of China Grant 2012AA02A520 (to X.-j.W.).

1. Dy GK, et al. (2009) Long-term survivors of metastatic colorectal cancer treated with systemic chemotherapy alone: A North Central Cancer Treatment Group review of 3811 patients, N0144. *Clin Colorectal Cancer* 8:88–93.
2. Ricci-Vitiani L, Pagliuca A, Palio E, Zeuner A, De Maria R (2008) Colon cancer stem cells. *Gut* 57:538–548.
3. Cho RW, Clarke MF (2008) Recent advances in cancer stem cells. *Curr Opin Genet Dev* 18:48–53.
4. O'Brien CA, Pollett A, Gallinger S, Dick JE (2007) A human colon cancer cell capable of initiating tumour growth in immunodeficient mice. *Nature* 445:106–110.
5. De Sousa E Melo F, et al. (2013) Poor-prognosis colon cancer is defined by a molecularly distinct subtype and develops from serrated precursor lesions. *Nat Med* 19: 614–618.
6. Guinney J, et al. (2015) The consensus molecular subtypes of colorectal cancer. *Nat Med* 21:1350–1356.
7. Sadanandam A, et al. (2013) A colorectal cancer classification system that associates cellular phenotype and responses to therapy. *Nat Med* 19:619–625.
8. Calon A, et al. (2015) Stromal gene expression defines poor-prognosis subtypes in colorectal cancer. *Nat Genet* 47:320–329.
9. Isella C, et al. (2015) Stromal contribution to the colorectal cancer transcriptome. *Nat Genet* 47:312–319.
10. Vermeulen L, et al. (2010) Wnt activity defines colon cancer stem cells and is regulated by the microenvironment. *Nat Cell Biol* 12:468–476.
11. Todaro M, et al. (2014) CD44v6 is a marker of constitutive and reprogrammed cancer stem cells driving colon cancer metastasis. *Cell Stem Cell* 14:342–356.
12. Lotti F, et al. (2013) Chemotherapy activates cancer-associated fibroblasts to maintain colorectal cancer-initiating cells by IL-17A. *J Exp Med* 210:2851–2872.
13. Calon A, et al. (2012) Dependency of colorectal cancer on a TGF-β-driven program in stromal cells for metastasis initiation. *Cancer Cell* 22:571–584.
14. Calon A, Tauriello DV, Batlle E (2014) TGF-beta in CAF-mediated tumor growth and metastasis. *Semin Cancer Biol* 25:15–22.
15. Keith B, Johnson RS, Simon MC (2011) HIF1α and HIF2α: Sibling rivalry in hypoxic tumour growth and progression. *Nat Rev Cancer* 12:9–22.
16. Plaks V, Kong N, Werb Z (2015) The cancer stem cell niche: How essential is the niche in regulating stemness of tumor cells? *Cell Stem Cell* 16:225–238.
17. Cao D, et al. (2009) Expression of HIF-1alpha and VEGF in colorectal cancer: Association with clinical outcomes and prognostic implications. *BMC Cancer* 9:432.
18. Rasheed S, et al. (2009) Hypoxia-inducible factor-1alpha and -2alpha are expressed in most rectal cancers but only hypoxia-inducible factor-1alpha is associated with prognosis. *Br J Cancer* 100:1666–1673.
19. Todaro M, et al. (2007) Colon cancer stem cells dictate tumor growth and resist cell death by production of interleukin-4. *Cell Stem Cell* 1:389–402.
20. Ibrahim EE, et al. (2012) Embryonic NANOG activity defines colorectal cancer stem cells and modulates through AP1- and TCF-dependent mechanisms. *Stem Cells* 30: 2076–2087.
21. Saigusa S, et al. (2009) Correlation of CD133, OCT4, and SOX2 in rectal cancer and their association with distant recurrence after chemoradiotherapy. *Ann Surg Oncol* 16:3488–3498.
22. Merlos-Suárez A, et al. (2011) The intestinal stem cell signature identifies colorectal cancer stem cells and predicts disease relapse. *Cell Stem Cell* 8:511–524.
23. Wilson WR, Hay MP (2011) Targeting hypoxia in cancer therapy. *Nat Rev Cancer* 11: 393–410.
24. Deng Y, et al. (2015) High SLFN11 expression predicts better survival for patients with KRAS exon 2 wild type colorectal cancer after treated with adjuvant oxaliplatin-based treatment. *BMC Cancer* 15:833.
25. Hanahan D, Coussens LM (2012) Accessories to the crime: Functions of cells recruited to the tumor microenvironment. *Cancer Cell* 21:309–322.
26. Su S, et al. (2018) CD10$^{+}$GPR77$^{+}$ cancer-associated fibroblasts promote cancer formation and chemoresistance by sustaining cancer stemness. *Cell* 172:841–856.e16.
27. Nagaraju GP, Bramhachari PV, Raghu G, El-Rayes BF (2015) Hypoxia inducible factor-1α: Its role in colorectal carcinogenesis and metastasis. *Cancer Lett* 366:11–18.
28. Varnat F, Siegl-Cachedenier I, Malerba M, Gervaz P, Ruiz i Altaba A (2010) Loss of WNT-TCF addiction and enhancement of HH-GLI1 signalling define the metastatic transition of human colon carcinomas. *EMBO Mol Med* 2:440–457.
29. Douard R, et al. (2006) Sonic Hedgehog-dependent proliferation in a series of patients with colorectal cancer. *Surgery* 139:665–670.
30. Scarpa M, Scarpa M (2016) Hedgehog signaling in colorectal cancer: A spiny issue gets smoothened. *Transl Cancer Res* 5:S1051–S1054.
31. Barrier A, et al. (2006) Stage II colon cancer prognosis prediction by tumor gene expression profiling. *J Clin Oncol* 24:4685–4691.
32. Smith JJ, et al. (2010) Experimentally derived metastasis gene expression profile predicts recurrence and death in patients with colon cancer. *Gastroenterology* 138:958–968.
33. Dalerba P, et al. (2016) CDX2 as a prognostic biomarker in stage II and stage III colon cancer. *N Engl J Med* 374:211–222.
34. Serova M, et al. (2015) Effects of TGF-beta signalling inhibition with galunisertib (LY2157299) in hepatocellular carcinoma models and in ex vivo whole tumor tissue samples from patients. *Oncotarget* 6:21614–21627.
35. Bhola NE, et al. (2013) TGF-β inhibition enhances chemotherapy action against triple-negative breast cancer. *J Clin Invest* 123:1348–1358.
36. Calone I, Souchelnytskyi S (2012) Inhibition of TGFβ signaling and its implications in anticancer treatments. *Exp Oncol* 34:9–16.
37. Gonnissen A, Isebaert S, Haustermans K (2015) Targeting the Hedgehog signaling pathway in cancer: Beyond smoothened. *Oncotarget* 6:13899–13913.
38. Johnson WE, Li C, Rabinovic A (2007) Adjusting batch effects in microarray expression data using empirical Bayes methods. *Biostatistics* 8:118–127.